A High-Speed Measurement Technique for the Ohmic Resistance of Lithium-Ion Batteries

Muhammad Sheraz [1] and Woojin Choi [1]
[1] Department of Electrical Engineering, Soongsil University, Seoul 06978, South Korea

***Abstract*--Lithium-ion batteries are gaining more attention in the rapidly growing industry of electrical vehicles (EVs). Moreover, a lot of efforts are put by the industry to reuse retired EVs batteries in energy storage systems (ESS). To achieve optimal performance of the repurposed xEVs batteries in ESS, they should be similar in characteristic such as capacity, State of Health (SOH) and Remaining Useful Life (RUL). This makes the battery grading techniques to play a crucial role in it. Ohmic resistance measurement is a convenient way to evaluate the battery aging. However, conventional Electrochemical Impedance Spectroscopy (EIS) methods to measure ohmic resistance require complex curve fitting procedures while some others conventional methods are not much accurate. This research proposes a high-speed technique to measure ohmic resistance directly without using these curve fitting procedures. A Combined Phased Multi-Sine (CPMS) excitation is used to perturb the battery in specific frequency band. The require perturbation time is just 1 sec and ohmic resistance is measured using two impedance values. This makes the proposed technique several times faster than conventional EIS methods. The accuracy is verified by performing experiments on three types of Li-ion batteries. The obtain results shows less than 0.15% difference with reference conventional EIS method. This technique is suitable for grading mass xEVs batteries by evaluating their aging.**

***Index Terms*—Electric Vehicles (EVs), Battery Aging. Combine Phased Multi-Sine (CPMS) Perturbation, Electrochemical Impedance Spectroscopy (EIS), Digital Lock-in Amplifier (DLIA), Lithium-Ion Battery (LIB), Ohmic Resistance.**

I. INTRODUCTION

Over the past few decades, significant efforts are made by humanity to combat the climate change. The use of fossil fuel-powered engines in industrial and transportation activities is one of the primary global warming contributors. These environmental and non-sustainability concerns have led to an increase in the adaptation of renewable energy resources and electric vehicles (EVs) across the globe [1][2]. In EVs and energy storage systems (ESS), lithium-ion batteries (LIB) are commonly used due to their efficiency, high energy density, long lifespan, and affordability [3]. Typically for EVs batteries, when the capacity drops by 20% of nominal value, it is considered as an end of life (EOL) [4][5]. However, serving the first in EVs, still a battery can store a significant amount of energy [6]. These retired batteries are used in repurposed system for second-life application such as in ESS. Based on the power and energy requirement, second life batteries (SLBs) are combined in different configurations in these repurposed systems. However, to ensure the performance optimization of the repurposed system, each battery should have similar characteristics in terms of capacity, State of Health (SOH) and Remaining Useful Life (RUL) [7].

There are various chemical and electrochemical processes occur inside a battery. Therefore, the aging phenomenon of a battery begins once it is manufactured. In case of LIB, aging results from binder decomposition, depletion of electrolyte, corrosion of the current collector, microcracks and gas evolution [9]. However, it is quite challenging to clearly distinguish these factors and identify particular aging characteristics. Instead, it is more convenient to measure the ohmic resistance R_s to evaluate aging of LIB. Since, it is widely known that ohmic resistance R_s is closely linked with the capacity fading, and SOH of a battery. Ohmic resistance Rs increases as the battery undergoes the degradation processes resulting in decrease of the battery capacity and SOH [10]. Therefore, it is used to depict the battery aging. Further, there are various methods to measure the ohmic resistance Rs. One way is to measure DC internal resistance (DCIR) through a voltage drop while DC load is connected. However, due to imposition of different contributing phenomenon, it is difficult to separate pure ohmic resistance R_s from the DCIR measured. Another method is the Electrochemical Impedance Spectroscopy (EIS) which provides a detailed understanding of internal electrochemical processes, the equivalent circuit model (ECM) parameters are extracted after performing the EIS test. However, it requires a long-time duration to perform an EIS test and extract ECM parameters by applying curve fitting procedures. Therefore, it is not practical for mass xEVs batteries testing. Another simple technique in which 1kHz AC signal is used to directly measure the impedance of the battery. The impedance measured is termed as ohmic resistance R_s under the assumption that 1kHz impedance point lies close to the Nyquist impedance plot zero-crossing. Since, the impedance of the battery at 1kHz is not necessary to be an ohmic resistance R_s. Therefore, the measurement results of this method are inherently unreliable and inaccurate.

In this paper, a high-speed technique is used to directly measure the ohmic resistance R_s of a battery accurately. A Combined Phase Multi-Sine (CPMS) excitation signal is used to perturb the battery for a narrow frequency band in which ohmic resistance R_s appears. It computes the ohmic resistance R_s directly using two impedance points and without additional curve fitting software. The proposed method accurately calculates the real axis zero crossing of the Nyquist impedance plot regardless of the battery type along with short measurement time. Based on this method,

a fast ohmic resistance R_s measurement hardware is fabricated. The accuracy and validity of the proposed technique is verified by comparing the measurement results with available commercial EIS instrument.

The paper is organized as: Ohmic resistance R_s measurement using conventional methods are discussed in section II. The methodology of proposed technique is explained in section III, hardware and software framework for the experiment are described in section IV, experimental results acquired are discussed in section V and the last section is used to conclude the work.

II. Conventional Methods

The conventional methods to measure the ohmic resistance R_s are explained below.

A. DCIR Method

In this method, DCIR is measured through a voltage drop across the battery while DC load is applied to the battery. Various factors are identified in the literature which contribute to this drop in voltage at different timescales. Randles battery model is shown in Fig.1. In Fig. 2b, an instantaneous voltage drop appear initially is due to ohmic resistance R_s, after few seconds the drop in voltage is due to double layer capacitance C_d and charge transfer resistance R_{ct}. In last, the shallow voltage drop is due to polarization resistance and decrease of SOC as a result of discharging [11].

$$DCIR = \frac{\Delta V}{\Delta I} \quad (1)$$

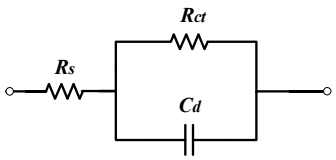

Fig. 1. Randles equivalent circuit model

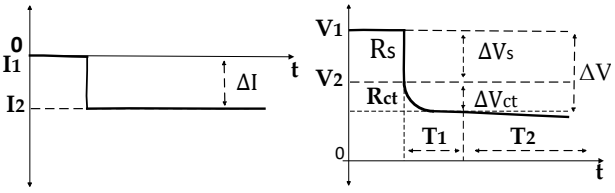

(a) (b)

Fig. 2. (a) Current response of a battery for load connected. (b) Voltage response of a battery to connected load.

The disadvantage of this approach is incorporating resistances from various sources which make it impossible to isolate pure ohmic resistance R_s from the DCIR measurement.

B. Electrochemical Impedance Spectroscopy (EIS)

Conventional EIS is a commonly used technique to get a detail information about the battery electrochemical processes. In Fig. 3, the complete EIS process to measure ohmic resistance R_s is illustrated. A sweep sinusoidal excitation is applied for a wide frequency band to perturb the battery, and response of the battery is acquired. The impedance spectrum is obtained after processing the battery response. Curve fitting procedures are applied to calculate ohmic resistance R_s and other ECM parameters [12].

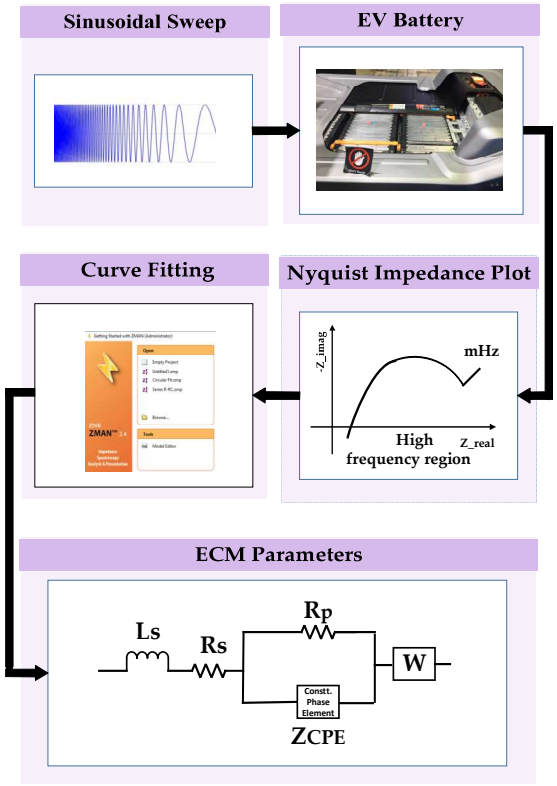

Fig. 3. Flowchart of conventional electrochemical impedance spectroscopy (EIS) and extraction of ECM parameters.

Although EIS is a reliable and accurate technique to measure the battery ohmic resistance R_s. However, the impedance is measured over a wide frequency range usually from Several kHz to mHz. Therefore, the measurement time to extract ohmic resistance R_s is quite high. The measurement time of conventional EIS is given by (2) [12].

$$T_{EIS} = \frac{1}{f_1} + \frac{1}{f_2} + \frac{1}{f_3} + \cdots + \frac{1}{f_n} \quad (2)$$

Where T_{EIS} is the time required to perform an EIS test and f_1, f_2, f_3.... f_n are the frequencies in measurement spectrum.

Secondly, Ohmic resistance R_s is not calculated directly. Rather, a curve fitting procedure is required for extracting the ECM parameters which itself is a complex and time-consuming process.

C. 1kHz AC Impedance Method

A 1kHz AC excitation signal is used to perturb the battery and measure the AC impedance of the battery. Equation (3) and (4) represents the response of the battery, the AC impedance is calculated using (5) [13].

$$I_r = I_m \sin(2000\pi t + \Phi_i) + I_{DC} \quad (3)$$

$$V_r = V_m \sin(2000\pi t + \Phi_v) + V_{DC} \quad (4)$$

$$Z_{ac} = \frac{V_r}{I_r} \quad (5)$$

$$Z_{ac} = R + jX \quad (6)$$

Where I_r, V_r, I_m, V_m, Φ_i, and Φ_v is the current response, voltage response, amplitudes, and phase shifts respectively. Z_{ac}, R and X is the AC impedance, resistive and reactive component respectively.

The same concept is used by HIOKI battery tester to measure ohmic resistance R_s. Although, measuring ohmic resistance R_s by 1kHz AC signal is quick and simple approach. However, they assume that 1kHz impedance lies close to the real axis zero crossing point on the Nyquist impedance plot. Since the 1kHz impedance location varies for different type of batteries as shown in Table I. Therefore, this assumption is not always valid. In Table I, the ohmic resistance R_s listed for numerous batteries is well below the 1kHz frequency range. Thus, measuring 1kHz impedance and considering it as ohmic resistance R_s is inaccurate and coincidental approach.

TABLE I
VARIETY OF BATTERIES WITH THEIR RESPECTIVE FREQUENCY BAND IN WHICH OHMIC RESISTANCE APPEARS

Battery Model	Frequency band in which ohmic resistance R_s appears (Hz)	Remarks
Automotive Li-ion Cells	1000	Below
Samsung INR18650	1000 – 500	Between
Valance 12-XP battery	500	Below
Samsung SM3 ZE battery pack	333 – 250	Between
Samsung INR18650 (4s7p)	333 – 250	Between
Bexel-158309	250 – 143	Between

III. PROPOSED TECHNIQUE OF OHMIC RESISTANCE MEASUREMENT

In proposed work, the battery is perturb using Combined Phased Multi-Sine (CPMS) signal for the frequency range in which ohmic resistance R_s of a battery appears. Instead of sinusoidal sweep excitation to perturb the battery with one frequency signal after another, all the frequency content are superimposed in a combined signal which reduce the measurement time. Further, as the ohmic resistance R_s appears in high frequency range. Therefore, wideband perturbation from several kHz to mHz is avoided. Hence, the perturbation range selected is from 1kHz to 100 Hz which further reduces the measurement time. The mentioned range is finalized after substantial literature review on ohmic resistance R_s concluded in Table I.

In a Combined Multi-Sine Signal (CMSS), all the frequency components are added up and the time period of the combined signal is equal to the lowest spectral component. However, if the signals are combined without modification, the resulting signal has very high crest factor (CF). As the EIS test should be performed under steady state condition with charge variation to be less than 5% of nominal battery capacity. Therefore, the CF of the combined signal should be optimized to ensure that battery is in steady state. Various methods are suggested in the literature to optimize the CF. The most suitable approach for proposed frequency range is using equally spaced frequency components with Schroder's phases are inserted. The combined signal obtained is term as CPMS having optimized CF and high Signal-to-Noise Ratio (SNR). The acquired CPMS is represented by (7) and (8).

$$E_{pms}[n] = \sum_{k=1}^{M} A_k \,.\, sin\left(\frac{2\pi n}{N_k} + \theta_k\right) \quad (7)$$

$$\theta_k = \frac{(k-k^2)\pi}{M} \quad (8)$$

$$f_s = N_k . f \quad (9)$$

Where E_{pms} is the CPMS, A_k is the amplitude, ϑ_k are the Schroeder's phases, N_k are the total number of samples, n is discrete time variable, k is an integer value, M is the number of combined frequency component, f_s and f are the sampling and actual frequency of each frequency component.

The time period of CPMS is equal to the lowest frequency component. Therefore, the measurement speed of proposed is technique is high, the time period of proposed CPMS signal is given by (10).

$$T_{Proposed} = \frac{1}{f_{100Hz}} \quad (10)$$

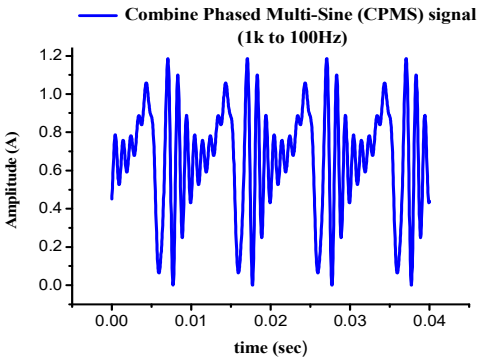

Fig. 4. Proposed Combined Phase Multi-Sine (CPMS).

The earlier CPMS mentioned is used to perturb the battery. The response is detected and processed through Digital Lock-in Amplifier (DLIA). Individual frequency component is extracted by the DLIA, and corresponding impedance spectrum is calculated. The proposed technique uses two impedance values to calculate ohmic resistance R_s. As shown in Fig. 5, two impedance points, Z_1 and Z_2, are selected above and below the real axis zero crossing of Nyquist impedance plot. Since, the impedance values Z_1 and Z_2 are not far from the real axis zero-crossing. Therefore, the following approach is used to calculate ohmic resistance R_s.

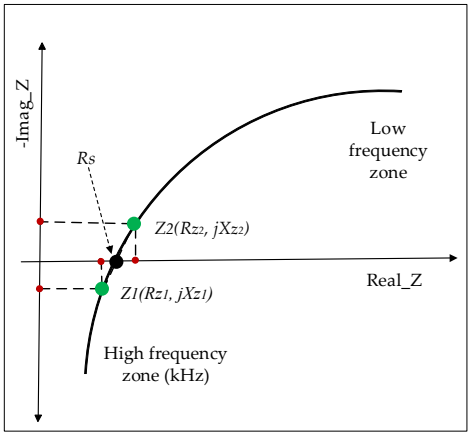

Fig. 5. Proposed technique to measure ohmic resistance R_s.

$$Z_1 = R_{z1} + jX_{z1} \quad \& \quad Z_2 = R_{z2} + jX_{z2} \tag{11}$$

$$X_z - X_{z1} = \left(\frac{X_{z2}-X_{z1}}{R_{z2}-R_{z1}}\right).(R_z - R_{z1}) \tag{12}$$

$$X_z = \left(\frac{X_{z2}-X_{z1}}{R_{z2}-R_{z1}}\right) \times (R_z - R_{z1}) \tag{13}$$

Where R_{z1}, jX_{z1}, R_{z2} and jX_{z2} represents the real and imaginary components of the chosen impedance values Z_1 and Z_2. R_Z and X_Z is the real and imaginary part of arbitrary impedance point on the Nyquist impedance plot respectively. As the above (13) is equated to zero, then arbitrary real part R_z=R_s. Equation (14) is the ohmic resistance R_s in terms of selected impedance values Z_1 and Z_2.

$$R_s = R_{z1} - X_{z1}.\left(\frac{R_{z2}-R_{z1}}{X_{z2}-X_{z1}}\right) \tag{14}$$

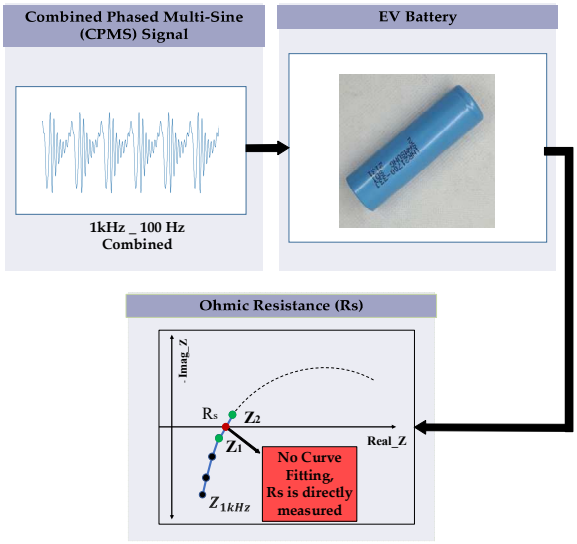

Fig. 6. Procedure followed by propososed technique to measure ohmic resistance R_s.

The procedure followed by proposed technique is describe in Fig. 6. By comparing it with the conventional EIS (shown in Fig. 3). The proposed technique doesn't require any curve fitting procedure. Ohmic resistance R_s of the battery is directly measured by simply using (14). Since, the CPMS is used for battery perturbation in frequency range 1kHz to 100Hz. Therefore, the proposed technique is multiple times faster than conventional EIS.

IV. PROPOSED TECHNIQUE'S HARDWARE AND SOFTWARE FRAMEWORK

The block diagram of the hardware setup is shown in Fig. 8 . The main hardware setup consists of DSP (FRDMK64F) for data processing, perturbation generation and controlling circuit, sensing, and conditioning circuit for reading the response of the battery. It is controlled from the PC and the user can communicate with hardware using LabVIEW based graphical user interface (GUI). By clicking the START button on the LabVIEW GUI, a CPMS signal is generated to perturb the battery. The battery response is read back through internal ADCs of FRDMK64F in connection with sensing and conditioning circuit.

The algorithms based on DLIA are implemented in FRDMK64F to calculate the ohmic R_s of the battery. The complete block diagram of DSP codes with LabVIEW based GUI is shown in Fig. 7, and block diagram of DLIA is shown in Fig. 9.

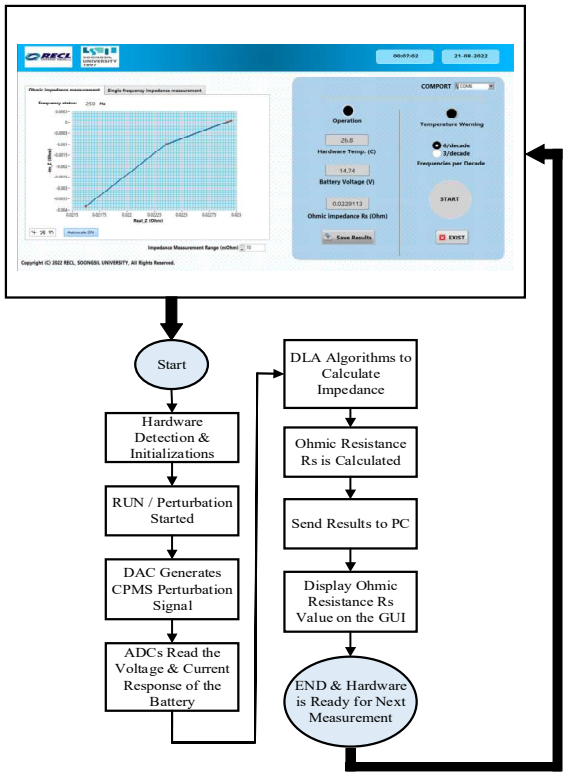

Fig. 7. LabVIEW GUI and flowchart of algorithms to measure ohmic resistance R_s

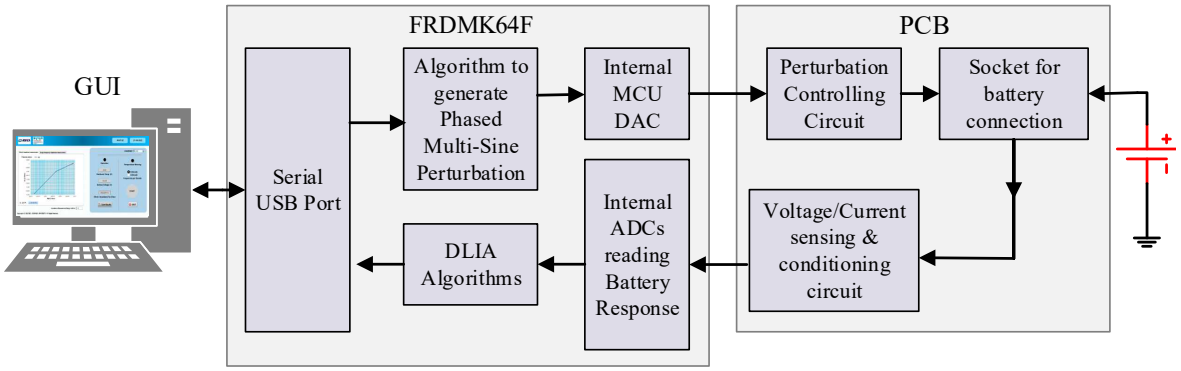

Fig. 8. Block diagram of hardware.

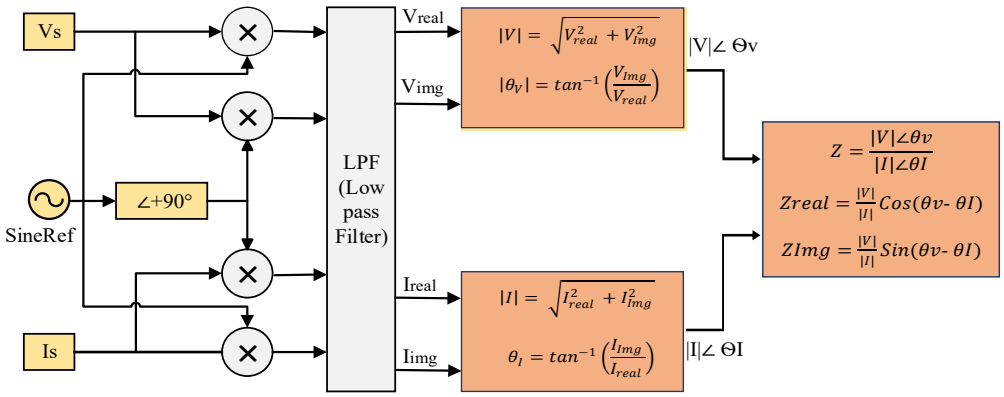

Fig. 9. Digital lock-in amplifier (DLIA) block diagram.

V. EXPERIMENTAL VALIDATION AND DISCUSSION

In this section, experiments are performed to verify the accuracy and validity of the proposed technique. The hardware setup used for the demonstration is shown in the Fig. 10 . The GUI developed in LabVIEW is open on laptop which is connected to hardware module using a Type-B USB cable. Since, the ohmic resistance R_s is quite small. Therefore, battery under test is connected to hard module using four-wire kelvin connection to eliminate the error caused by lead resistances. The specification of Li-ion batteries used in the experiment are listed in Table II.

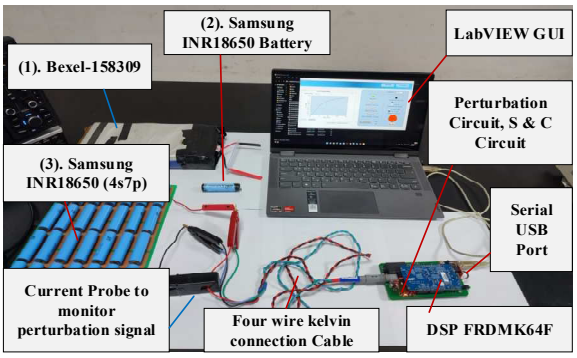

Fig. 10. Hardware setup for experimentation

TABLE II
SPECIFICATION OF BATTERIES

S.No	Battery Name	Configuration	Nominal Voltage (V)	Capacity (Ah)
1	Bexel-158309	4s	14.80	32
2	Samsung INR18650	Single Cell	3.65	2.750
3	Samsung INR18650	4s7p	14.60	19.95

In the experimental validation, ohmic resistance R_s of listed batteries is measured through EISLV instrument by Batronics Co.Ltd, 1kHz AC impedance method and proposed technique. The results obtained are plotted in Fig. 11, Fig. 12, and Fig. 13 respectively. It can be seen that impedance plots (1kHz to 100 Hz) obtain through proposed technique are well matched with that of commercially available instrument. For ECM parameter extraction, a curve fitting software ZMAN is applied to the impedance spectrum data obtain through EISLV. The Ohmic resistance R_s measured through EISLV (after curve fitting), 1kHz AC impedance method and proposed technique are concluded in Table III, Fig. 14, and Fig. 15.

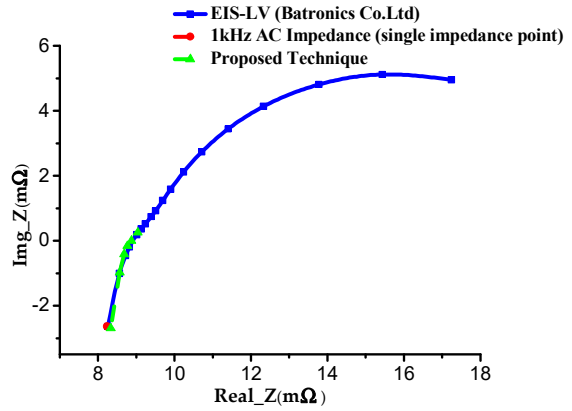

Fig. 11. Nyquist impedance plot comparison of Bexel-158309 obtain through proposed technique, commercial EISLV, and 1kHz impedance method.

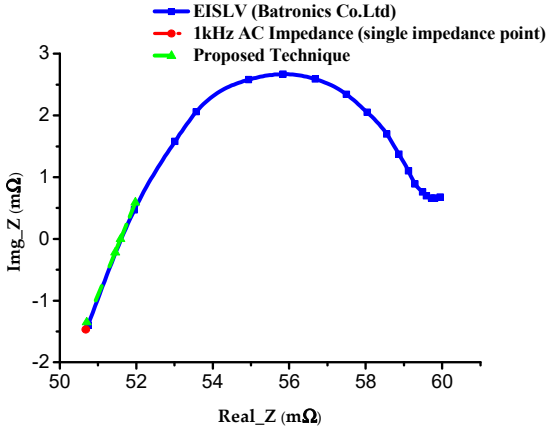

Fig. 12. Nyquist impedance plot comparison of Samsung INR18650 (single cell) obtain through proposed technique, commercial EISLV, and 1kHz impedance method.

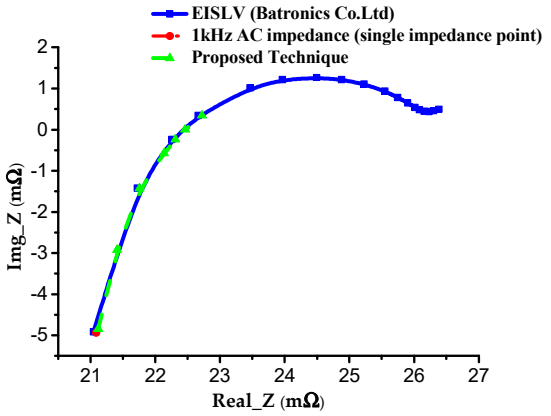

Fig. 13. Nyquist impedance plot comparison of Samsung INR18650 (4s7p) obtain through proposed technique, commercial EISLV, and 1kHz impedance method.

TABLE III
OHMIC RESISTANCE MEASURED THROUGH PROPOSED TECHNIQUE, 1KHZ AC IMPEDANCE METHOD AND EISLV

Fast Ohmic Resistance R_s Measurement			
Battery Model	EISLV by Batronics Co.Ltd (mΩ)	1kHz AC Impedance Method (mΩ)	Proposed Technique (mΩ)
Bexel-158309	8.314	7.813	8.326
Samsung INR18650	51.795	51.127	51.853
Samsung INR18650	23.261	21.953	23.276

In Fig. 14, the ohmic resistance Rs results obtained for Bexel 158309, Samsung INR18650, and Samsung INR18650 (4s7p) are plotted on a bar chart. It expressed that proposed technique accurately measure the ohmic resistance Rs. In Fig. 15, the percentage error of 1kHz AC impedance and proposed method are compared to reference EISLV. The 1kHz AC signal method gives an error of more than 5% for Bexel 158309 and Samsung INR18650 (4s7p). However, for all tested batteries, the percentage difference recorded in measurement of proposed technique is less than 0.15%.

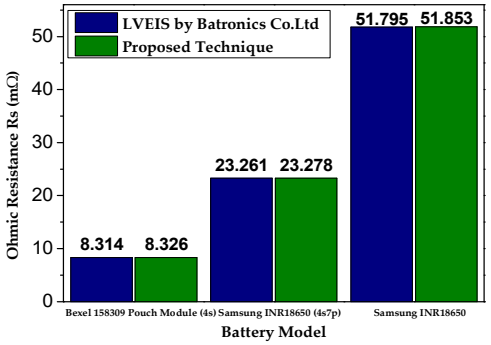

Fig. 14. Comparison of ohmic resistance values obtain through proposed technique and EISLV.

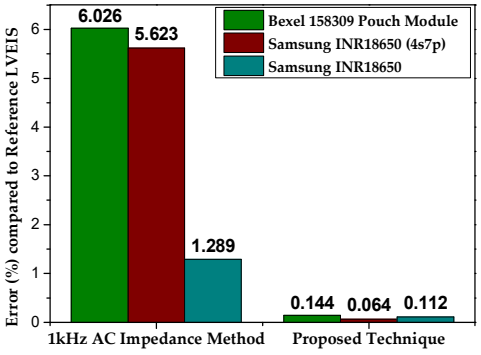

Fig. 15. Percentage % error comparison of proposed technique and 1kHz impedance method, the reference is commercial EISLV by Batronics Co.Ltd.

In Table IV below, the measurement time of proposed technique is compared with conventional EIS method. The proposed technique perturbs the battery just for 1 sec to measure ohmic resistance R_s of a battery. In contrast, the battery perturbation time for the conventional EIS is 27 to 87 sec which is quite longer than proposed technique. Therefore, in comparison with conventional EIS, the measurement speed of proposed is multi-times faster.

The proposed technique measure ohmic resistance R_s directly and display value on the LabVIEW GUI instantly after the experiment completes. Unlike conventional EIS, there is no need to apply complex curve fitting procedures. Therefore, the benefits of the proposed technique make it more practical option for mass testing and grading of LIB than conventional methods.

TABLE IV
PERTURBATION TIME FOR PROPOSED TECHNIQUE AND CONVENTIONAL EIS METHOD

Method	Perturbation Time of Battery (Sec)	Remarks
Convention EIS	26 to 87	1 Hz to 1kHz 0.1 Hz to 1kHz
Proposed Technique	1.0	Fixed

CONCLUSION

In this work, a high-speed technique is proposed to measure the ohmic resistance of Li-ion battery. It involves the development of hardware setup and algorithms based on the proposed technique. The accuracy and validity are verified through experiments and the results obtained are compared with those of commercial EIS instrument. The experimental results obtained shows that proposed technique has less than 0.15% difference in measurements of ohmic resistance with reference commercial EIS instrument, whereas the conventional 1kHz AC impedance method has more than 5% error. As the proposed technique perturb the battery using Combined Phased Multi-Sine (CPMS) signal in a specified narrow frequency band (1kHz to 100 Hz) in which ohmic resistance of a battery appears. Therefore, the perturbation time for the battery is just 1 sec and the measurement speed is multiple times faster than conventional EIS methods. Furthermore, no curve fitting software is required. Rather, it directly measures the ohmic resistance and the results are displayed on LabVIEW GUI instantly after the experiment completes. Therefore, it is most suitable solution for aging and grading Li-ion batteries.

ACKNOWLEDGMENT

The authors would like to acknowledge the National Research Foundation (NRF) of the Republic of Korea (ROK) for funding this research under Grant No. NRF2021R1A2C1011504 “Research on the High-Speed Multichannel Impedance Spectroscopy Technique for Battery Performance Evaluation”.

REFERENCES

[1] C. Vidal, O. Gross, R. Gu, P. Kollmeyer and A. Emadi, "xEV Li-Ion Battery Low-Temperature Effects—Review," in IEEE Transactions on Vehicular Technology, vol. 68, no. 5, pp. 4560-4572, May 2019, doi: 10.1109/TVT.2019.2906487.

[2] X. He, T. Maxwell and M. E. Parten, "Development of a Hybrid Electric Vehicle With a Hydrogen-Fueled IC Engine," in IEEE Transactions on Vehicular Technology, vol. 55, no. 6, pp. 1693-1703, Nov. 2006, doi: 10.1109/TVT.2006.878609.

[3] R. Xiong, Y. Zhang, J. Wang, H. He, S. Peng and M. Pecht, "Lithium-Ion Battery Health Prognosis Based on a Real Battery Management System Used in Electric Vehicles," in IEEE Transactions on Vehicular Technology, vol. 68, no. 5, pp. 4110-4121, May 2019, doi: 10.1109/TVT.2018.2864688.

[4] J. -M. Timmermans et al., "Batteries 2020 — Lithium-ion battery first and second life ageing, validated battery models, lifetime modelling and ageing assessment of thermal parameters," 2016 18th European Conference on Power Electronics and Applications (EPE'16 ECCE Europe), Karlsruhe, Germany, 2016, pp. 1-23, doi: 10.1109/EPE.2016.7695698.

[5] T. Montes, M. Etxandi-Santolaya, J. Eichman, V. J. Ferreira, L. Trilla, and C. Corchero, “Procedure for Assessing the Suitability of Battery Second Life Applications after EV First Life,” Batteries, vol. 8, no. 9, p. 122, Sep. 2022, doi: 10.3390/batteries8090122.

[6] D. Strickland, L. Chittock, D. A. Stone, M. P. Foster and B. Price, "Estimation of Transportation Battery Second Life for Use in Electricity Grid Systems," in IEEE Transactions on Sustainable Energy, vol. 5, no. 3, pp. 795-803, July 2014, doi: 10.1109/TSTE.2014.2303572.

[7] E. Hossain, D. Murtaugh, J. Mody, H. M. R. Faruque, M. S. Haque Sunny and N. Mohammad, "A Comprehensive Review on Second-Life Batteries: Current State, Manufacturing Considerations, Applications, Impacts, Barriers & Potential Solutions, Business Strategies, and Policies," in IEEE Access, vol. 7, pp. 73215-73252, 2019, doi: 10.1109/ACCESS.2019.2917859.

[8] Decheng Zhao, Zhen Zhang, Jinghui Ren, Yuanyuan Xu, Xiangyu Xu, Jian Zhou, Fei Gao, Hao Tang, Shupei Liu, Zhoulu Wang, Di Wang, Yutong Wu, Xiang Liu, Yi Zhang,

[9] Fe2VO4 nanoparticles on rGO as anode material for high-rate and durable lithium and sodium ion batteries, Chemical Engineering Journal, Volume 451, Part 3, 2023, 138882, ISSN 1385-8947,https://doi.org/10.1016/j.cej.2022.138882.

[10] A. El Mejdoubi, H. Chaoui, H. Gualous, P. Van Den Bossche, N. Omar and J. Van Mierlo, "Lithium-Ion Batteries Health Prognosis Considering Aging Conditions," in IEEE Transactions on Power Electronics, vol. 34, no. 7, pp. 6834-6844, July 2019, doi: 10.1109/TPEL.2018.2873247.

[11] Anup Barai, Gael H. Chouchelamane, Yue Guo, Andrew McGordon, Paul Jennings,A study on the impact of lithium-ion cell relaxation on electrochemical impedance spectroscopy,Journal of Power Sources,Volume 280,2015,Pages 74-80,ISSN 0378-7753, https://doi.org/10.1016/j.jpowsour.2015.01.097.

[12] F. Farooq, A. Khan, S. J. Lee, M. Mahad Nadeem, and W. Choi, “A Multi-Channel Fast Impedance Spectroscopy Instrument Developed for Quality Assurance of Super-Capacitors,” Energies, vol. 14, no. 4, p. 1139, Feb. 2021, doi: 10.3390/en14041139.

[13] H.-G. Schweiger et al., “Comparison of Several Methods for Determining the Internal Resistance of Lithium Ion Cells,” Sensors, vol. 10, no. 6, pp. 5604–5625, Jun. 2010, doi: 10.3390/s1006056.